

Ab initio predictions for the effect of disorder and quaternary alloying on the half-metallic properties of selected Co₂Fe-based Heusler alloys

This article has been downloaded from IOPscience. Please scroll down to see the full text article.

2007 J. Phys.: Condens. Matter 19 326216

(<http://iopscience.iop.org/0953-8984/19/32/326216>)

View [the table of contents for this issue](#), or go to the [journal homepage](#) for more

Download details:

IP Address: 129.252.86.83

The article was downloaded on 28/05/2010 at 19:58

Please note that [terms and conditions apply](#).

***Ab initio* predictions for the effect of disorder and quarternary alloying on the half-metallic properties of selected Co₂Fe-based Heusler alloys**

Z Gercsi¹ and K Hono^{2,3}

¹ International Center for Young Scientists (ICYS), National Institute for Materials Science, Tsukuba 305-0047, Japan

² Magnetic Materials Center, National Institute for Materials Science, Tsukuba 305-0047, Japan

³ Graduate School of Pure and Applied Sciences, University of Tsukuba, Japan

E-mail: Gercsi.Zsolt@nims.go.jp

Received 25 April 2007

Published 17 July 2007

Online at stacks.iop.org/JPhysCM/19/326216

Abstract

Co₂Fe-based Heusler alloys possess high Curie temperatures and magnetization, therefore they are the most studied compositions for spintronics applications. Here we report *ab initio* calculations to investigate the effect of structural disorder on the theoretical spin polarization and magnetization in ternary Co_{2.25-x}Fe_{0.75+x}Si alloys. Quarternary Heusler alloys with substitution of Mn or Cr for Fe, and gradual replacement of Si by Al or Ga in the Co₂FeSi composition, were also studied. For high Fe concentration alloys, the Slater–Pauling rule is preserved if a small on-site Coulomb exchange is taken into account in the calculations. In such a case, the change in the total number of valence electrons by alloying was found to be an efficient way to tailor the half-metallic behavior with high resistance against structural disorder. The necessity of the on-site correlation in these alloys to the correct description of magnetic and electronic structure is also addressed.

(Some figures in this article are in colour only in the electronic version)

1. Introduction

As was investigated by Kübler *et al* [1], many of the Heusler alloys show metal-like band structures for the majority-spin electrons, with a discrete energy gap in the minority-spin electron states at the Fermi level (E_F). Spintronics is based on the idea of exploiting the unique physical features of the highly spin-polarized currents generated by these half-metals. Various spintronics device applications not only demand high spin polarization (P) but also high Curie temperature and magnetization.

Among many full-Heusler alloys, Co-based ones are the most promising candidates to fulfill these requirements. Besides Co₂MnSi [2, 3], Co₂FeSi [4, 5] has received the most interest

due to it having highest Curie temperature (>1100 K) of all known full-Heusler alloys, with an expected integer magnetic moment of $6.0 \mu_B$, derived from the Slater–Pauling rule [6], $M_s = Z - 24 (\mu_B)$, where Z is the number of valence electrons. However, theoretical calculations by Galanakis *et al* [6] using the local density approximation (LDA) method predicted a lower magnetic moment of only $5.3 \mu_B$ with no half-metallicity. Also, in early experimental studies, the magnetic moment of this composition was reported to be 5.6 and $5.9 \mu_B$ with a considerably high amount of disorder in the bulk samples [7, 8]. Therefore the Co_2FeSi had not attracted much research interest until a magnetic moment of $6.0 \mu_B$ was measured experimentally by Wurhmel *et al* [9], reflecting the validity of the Slater–Pauling rule on this compound. This result generated intensive theoretical work to explain the experimentally measured magnetization. Since the full-Heusler alloys are traditionally considered as ideal local magnetic moment systems, the LDA method is widely used to model the electronic structure of these alloys. However, including the electron–electron Coulomb repulsion energy (U) in the LDA model (LDA + U), the missing magnetic moment can be explained [10–13]. These works investigated the electronic structure and magnetic properties of Co_2FeSi within a wide interaction range of $U \approx 1.7$ – 4.5 eV and concluded that only a small strength of the Coulomb interaction (~ 2 eV) needs to be considered in order to find good agreement with experimental results. In such a case, the Co_2FeSi alloy is predicted to be half-metallic, with E_F lying close to the minimum energy of the conduction electron band.

A reduction in the total number of valence electrons by partial the replacement of the element Fe or Si by the elements Mn, Cr or Al is found to be an effective way to achieve a virtual shift of E_F within the half-metallic band gap [14–17]. For instance, the experimentally observed high tunneling magnetoresistance (TMR) effect of 175% at room temperature in the magnetic tunneling junction (MTJ) using a ferromagnetic electrode of equiatomic $\text{Co}_2\text{FeAl}_{0.5}\text{Si}_{0.5}$ [18] is related to the central position of the Fermi energy within the band gap. Similarly, the initial increase in P with x in the $\text{Co}_2\text{Fe}_{1-x}\text{Cr}_x\text{Si}$ alloy series is attributed to the same effect [17]. The alloying of Co_2FeSi to tune the position of E_F in the band gap by a moderate decrease in the total number of valence electrons may also be accomplished by:

- (i) changing the 2:1 relative fraction of Co to Fe atoms in the compound;
- (ii) quarternary substitution for the p-block element Si by Al or Ga;
- (iii) quarternary substitution for the d-block element Fe by Mn or Cr.

In this work, based on density-functional theory (DFT), we have used *ab initio* calculations to investigate the alloying effect on both the electronic structure and magnetic properties in the $\text{Co}_{2.25-x}\text{Fe}_{0.75+x}\text{Si}$ ternary alloys as well as in the $\text{Co}_2\text{Fe}_{1-x}\text{M}_x\text{Si}$ quarternary alloys with $M = \text{Mn}$ or Cr and in the $\text{Co}_2\text{FeSi}_{1-x}\text{P}_x$ quarternary alloys with $P = \text{Al}$ or Ga . Furthermore, the lower experimentally achieved TMR effect and experimentally observed spin polarization in the range of only $P = 0.5$ – 0.65 in actual Co-based alloys and thin films are supposed to be strongly related to the presence of structural disorder in the ferromagnetic electrode alloys. However, very few investigations on the effect of disorder have been reported so far [19–21]. Therefore, in this paper we have also focused on the effect of A2-, B2- and DO_3 -type disorders in these ordered alloys. These disorders were simulated using an A_2BC supercell composed of 16 atoms (eight A atoms, four B atoms and four C atoms) within the general gradient approximation (GGA) and GGA + U frameworks. The total energies of the disordered phases were compared to the $L2_1$ phase in order to examine the stability of that phase.

The goal of this work is not only to predict new alloys with half-metallic properties in the perfectly ordered $L2_1$ structure but also to select the most promising compositions or composition ranges where the half-metallicity is maintained against some structural disorder and compositional fluctuations.

2. Computational model

Ab initio calculations using the OpenMX free software package [22] were carried out to calculate both the density of states (DOS) and the magnetic properties. The DOS calculations have been performed on the basis of the density-functional theory (DFT) within the general gradient approximation (GGA) method. We also performed GGA + U calculations to account for the on-site electron–electron Coulomb interaction of the d electrons of Co, Fe, Mn and Cr elements. The pre-generated fully relativistic pseudo-potentials and the pseudo-atomic orbitals with a cutoff radius of 6.5 au were downloaded from the OpenMX website [22]. Basis orbitals were fixed to 2s 2p 1d for each element, with an energy cutoff of 180 Ryd for the numerical integrations, while the energy convergence criterion was set to 10^{-7} Hartree during the fitting procedure. The spin–orbit interaction was not considered in the calculations. Using these conditions, excellent reproducibility was confirmed on other previously reported full-Heusler alloys. The crystal structure of the $L2_1$ -ordered full-Heusler A_2BC alloy consists of four face-centered cubic (fcc) sublattices with A atoms at the 8c ($\frac{1}{4} \frac{1}{4} \frac{1}{4}$ and $\frac{1}{4} \frac{1}{4} \frac{3}{4}$) positions, B atoms at the 4b ($\frac{1}{2} \frac{1}{2} \frac{1}{2}$) positions and C atoms at 4a (0 0 0) positions in Wyckoff coordinates.

Initially, 16 atoms in the $L2_1$ unit cell composed of eight Co, four Fe and four Si atoms were taken for the self-consistency calculations considering the bulk Co_2FeSi alloy. For instance, in the series of $\text{Co}_2\text{FeSi}_{1-x}\text{Al}_x$, Al addition was carried out by gradual replacement of those four Si atoms by Al atoms. In such a way, replacement of one of the four Si atoms by an Al atom results in $x = 0.25$, while the addition of two Al atoms in the place of two Si atoms results in $x = 0.50$ etc in the $\text{Co}_2\text{FeAl}_x\text{Si}_{1-x}$ formula.

The effect of disorder was modeled in such a way that the position of Si and Al atoms was swapped by Fe atoms to simulate the B2-type disorder and the position of a Co atom was mixed by an Fe atom for the DO_3 -type disorder, respectively. The A2-type disorder was realized by the replacement of a Co atom by a single Si atom. Therefore the smallest amount of disorder that can be introduced was 12.5% for A2 or DO_3 -type and 25% for B2-type disorder. The same scheme was applied for every calculated alloy in this work.

It is important to emphasize that, using this computational model, the genuineness of these simulations on various disorders is rather limited due to the statistically randomly distributed nature of the disorder in real alloys. This model is based on a supercell (described above), hence a change in the position of two atoms in the unit cell means that their position is changed (and fixed!) in the same way in the bulk due to translation. In a sense, this can be considered as a superlattice structure. However in a real matter, the disorder appears at different sites in the bulk. Furthermore, in the quaternary compositions, the same amount of disorder can be realized by swapping different elements which may create different next-neighbor environment. In such cases, we always refer to the most stable one, considering the difference in the total energies (ΔE_{tot}) compared to the $L2_1$ structure, but it is emphasized in the text if there are significant differences between the variations.

Finally, the lattice parameters were fixed to the experimentally obtained values for the terminal alloys [8, 16, 17, 23] or interpolated assuming its linear dependence (Vegard’s law) on the concentration. Note that no geometry optimization (relaxation) was taken into account during the calculations.

3. Results and discussion

As was mentioned in the introduction, much effort has gone into research based on the LSDA method of calculating the electronic structure of full-Heusler alloys. This model predicted only 5.3–5.5 μ_B magnetization without half-metallic electronic structure but, by applying the

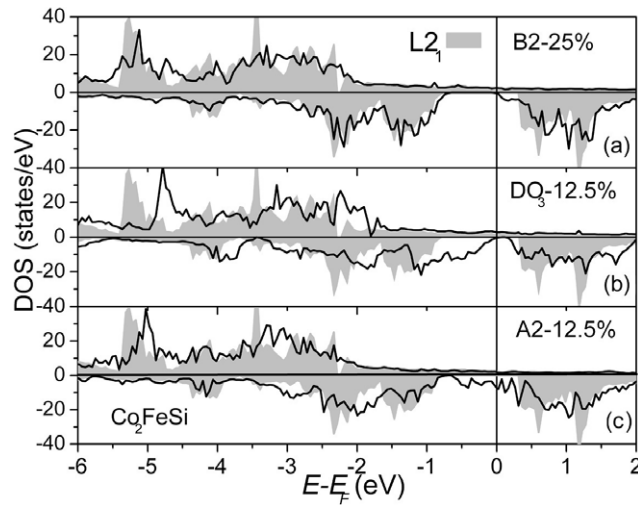


Figure 1. The total density of states (DOS) of Co_2FeSi alloy with B2 (a), DO_3 (b) and A2 (c) disorders, respectively. The $L2_1$ -ordered phase is also shown in grey for reference.

Hubbard model (either within the LDA + U or in the GGA + U theorem), the experimentally measured magnetic moment can be calculated. Although there are some works which estimate the value of the electron–electron interaction strength for 3d metals, there are no completely reliable schemes to calculate U in metals [24, 25]. However, using any value of U from 1.8 to 5 eV, the calculated value of M_s remains independently $6.0 \mu_B$ [9, 12, 14].

For the half-metallicity, U has a cardinal effect on the position of the band gap in the minority-spin electron states. We can generally say that the higher the Coulomb interaction that is considered, the higher the energies that the band gap is pushed toward. Nevertheless, using U values of the magnitude of ~ 2 eV, a reasonable agreement between the theoretical density of states (DOS) and the experimental photoelectron spectra can be found [14]. Therefore, in our calculations, the strength of the Coulomb interaction for the transition-metal elements was chosen arbitrary within the ~ 2 eV range, presuming that it increases with atomic number [26], namely $U_{\text{Cr}} = 1.8 < U_{\text{Mn}} = 1.9 < U_{\text{Fe}} = 2.0 < U_{\text{Co}} = 2.1$ eV. The calculations performed with these moderate values resulted in a better match with experiment for most of the cases, as we will explain below.

3.1. Ternary $\text{Co}_{2.25-x}\text{Fe}_{0.75+x}\text{Si}$ alloys

Here, we first present our result on the stoichiometric Co_2FeSi parent alloy, followed by the off-stoichiometric compositions with $x = 0$ and 0.5 . Figure 1(a) shows the spin-resolved density of states (DOS) of the Co_2FeSi phase for the completely $L2_1$ ordered and B2-type disordered structures calculated by GGA + U . The gap in the minority DOS around the Fermi energy reflects the half-metallicity of the compound. The lowest energy of the dispersed unoccupied d band in the minority electron states formed by both Co and Fe are about 0.3 eV above E_F . The introduction of 25% B2-type disorder by swapping the position of a Fe atom for a Si atom results in the appearance of new electronic states at E_F from the minimum side of the conduction band. This new peak at E_F is due to the change in the crystal field symmetry at the Co 8c and Fe 4a sites, which results in the additional splitting in the d orbitals. However, the overall magnetic moment is affected very little by this kind of disorder.

In order to establish the DO₃-type disorder, the Co atoms were swapped by Fe atoms. As is seen in figure 1(b), although 12.5% of disorder broadened the gap for the minority electrons at E_F , 100% spin polarization is still conserved. On the other hand, a consistent decrease in the total magnetic moment is observed due to the broken crystal field symmetry. The decrease in the total spin moment from 6.0 to 5.5 μ_B is because of the lowering in the M_t of the Fe atom on the 8c site from 3.16 to 2.45 μ_B , which is only partly compensated by the moderate increase in that of the Co atom on the 4a site from 1.54 to 1.95 μ_B . An average decrease of about 0.1 μ_B on each of the next-neighbor atoms is also observed. It must be noticed that the same decrease in total magnetization is also observed within the GGA theory from 5.66 to 5.13 μ_B by the introduction of the same disorder. Analysis of the partial DOS of the atoms in cell (not shown here) reflects that the shoulder which appeared from the valence band side and which shrank the band gap is mainly related to the 3d states of those swapped Co and Fe atoms. These newly appeared and disturbed states are rather localized and the perturbation of the electronic structure of the atoms on the next-neighbor and especially on the second-next-neighbor sites fades away. A further increase in disorder to 25% or above (not shown here) results in vanished half-metallicity due to the strong reduction of the band gap width. The magnetic moment of the structure is again found to be reduced to 5.5 μ_B .

When Co and Si atoms swap their sides (12.5% A2 disorder), the magnetization increases slightly to 6.15 μ_B , and no band gap in the minority-spin electron states exists (figure 1(c)). The interchange between the transition-metal elements is energetically more preferable than the Co–Si-type mixing due to the similar size and electronic structure of Fe and Co atoms, thus this is a highly unfavorable metastable state, at least at 0 K, which is confirmed by the relevant increase in ΔE_{total} . It must be noticed that an antiparallel configuration of the Co atom on the 4c site is also found with $-2.14 \mu_B$ magnetic moment, which results in $M_t = 5.0 \mu_B$; however, this arrangement had a consistently higher ($\Delta E_{\text{total}} \approx 0.3 \text{ eV}$) total energy minimum. Also, the half-metallicity (HM) is lost in both cases. Figure 2 summarizes the total magnetic moment together with the change in the total energy (ΔE_{total}) caused by the disorder. The total energy of the $L2_1$ phase is considered as the reference (most stable phase). We also indicate whether or not the spin polarization expected from the GGA + U calculations is 100% (yes) or smaller (no).

Partial replacement of cobalt ($x = 0$) or iron atoms ($x = 0.5$) in $\text{Co}_{2.25-x}\text{Fe}_{0.75+x}\text{Si}$ results in a change in the total number of valence electrons in the off-stoichiometric compounds. The Slater–Pauling rule should result in a total magnetic moment of 5.75 μ_B for the Fe-rich composition and 6.25 μ_B for the Co-rich composition; however, neither the GGA nor the GGA + U theory can predict the latter value. Not surprisingly, the shrinkage of the band gap in the minority density of states at E_F for the off-stoichiometric composition in figure 3 shows a similarity with the above-described DO₃-type disorder in the Co_2FeSi alloy. Again, the substituted Co atom carries a lower magnetic moment (1.8 μ_B) than the Fe atoms (3.2 μ_B) on the 4b site. The effect of various disorders for the off-stoichiometric compositions are summarized in figure 2; with higher Co content, the alloy is less stable against structural disorder than the Fe-rich counterpart. Also, the predicted total magnetic moment shows a strong dependence on both the disorder and the change in chemical composition. This behavior may explain the diversity of experimentally obtained results.

3.2. Quarternary $\text{Co}_2\text{Fe}_{1-x}\text{Mn}_x\text{Si}$ alloys

As was shown above, reducing the valence electrons in the Co_2FeSi is a feasible way to tailor the position of the Fermi level within the half-metallic band gap. Nevertheless, this decrease in the total number of valence electrons can also be made by the gradual substitution of the Y

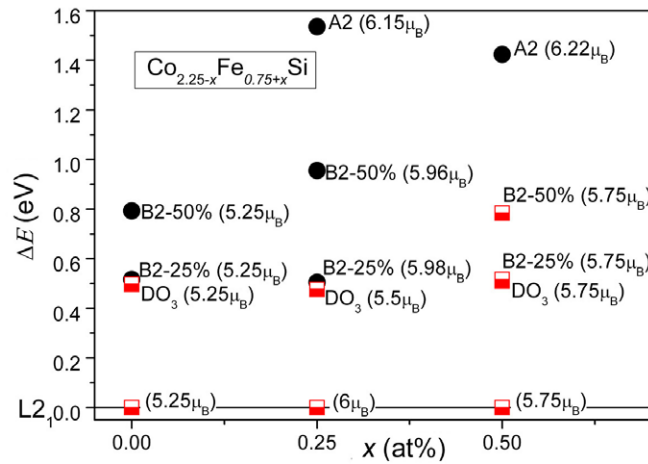


Figure 2. The effect of alloying and the effect of various disorders for the half-metallicity in $\text{Co}_{2.25-x}\text{Fe}_{0.75+x}\text{Si}$ alloys compared by their difference in total energy. The half-filled squares represent $P = 1$, while full circles indicate decreased spin polarization ($P < 1$) as a result of the calculations.

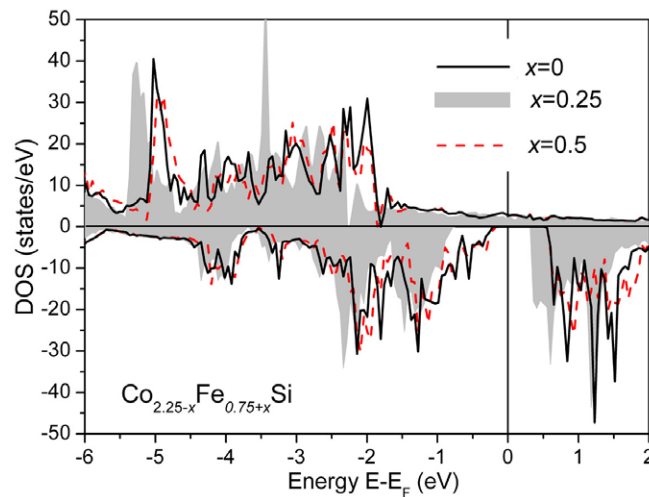


Figure 3. The total density of states (DOS) of $\text{Co}_{2.25-x}\text{Fe}_{0.75+x}\text{Si}$ alloys with $L2_1$ ordered structure. The gap in the minority states shrinks for off-stoichiometric compositions.

element (Fe) by another d-block element onto the same (4b) sublattice with a smaller number of valence electrons. In such a way, the DO_3 -type disorder may be depressed. The closest left neighbor of a Fe ($3d^64s^2$) atom is the Mn ($3d^54s^2$), with seven valence electrons, followed by the Cr ($3d^54s^1$) with six valence electrons. First, we investigate the effect of Mn quaternary alloying followed by the effect of Fe replacement by Cr in the Co_2FeSi . Experimental work performed by Balke *et al* [14] found a linear decrease in the total magnetization with Mn addition over the whole composition range of $L2_1$ -ordered $\text{Co}_2\text{Fe}_{1-x}\text{Mn}_x\text{Si}$ alloys, which reflects the validity of the Slater–Pauling rule in these compounds. This behavior is predictable

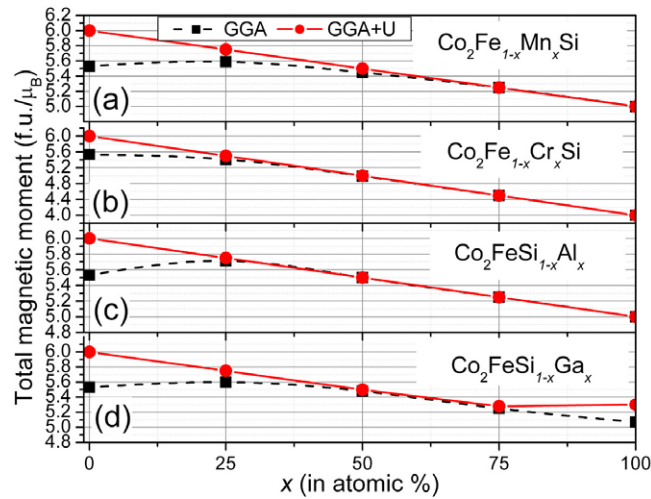


Figure 4. Calculated total magnetic moments expected from the GGA and GGA + U theories for Mn (a), Cr (b), Al (c) and Ga (d) added quaternary Co_2Fe -based alloys. The Coulomb repulsion corrected model reproduces the linear Slater–Pauling rule.

in the low-Fe-content region using the GGA theory, however only by a weak electron–electron interaction can the magnetization be explained in the high-Fe-content range ($0 \leq x < 0.75$), as shown in figure 4(a). In the latter, the half-metallic nature of the electronic structure is revealed. When the number of valence electrons is reduced on increasing x , the E_F is found to be deeper into the minority band gap. The Fermi energy is approximately in the middle of the gap, close to the equiatomic Fe and Mn concentration. For more Mn addition, the Fermi energy approaches the maximum of the valence electron band, and for $x = 1$ the E_F is at the edge of the half-metallic gap (see figure 5). This behavior presumes a stronger resistance of half-metallic against structural disorders for alloys with intermediate Mn and Fe concentrations ($0.25 \leq x \leq 0.75$) than for the terminal alloys ($x = 0$ and 1). This is similar to the Mn-free alloy, where the swapping of Co with Fe atoms in the $L2_1$ structure results in a decrease in M_t , while the Co–Si-type disorder increases the total magnetic moment but the half-metallicity is eliminated by both types of disorder for $x = 0.25$ (see figure 6). However, for the Co–Mn interchange, as well as for the complete B2-type disorder, the E_F is still found to be within the band gap. For more Mn addition to $x = 0.5$, the E_F moves toward the minimum side of the conduction band, thus in the presence of much B2 disorder the half-metallicity is not preserved. For higher Mn concentrations ($x = 0.75$ and for $x = 1$), only the completely $L2_1$ -ordered structure exhibits half-metallic properties and any type of disorder lowers the spin polarization. The total magnetization is very unstable and shows strong fluctuation with structural dependences in these cases. Even if a small strength of electron–electron interaction is considered in these low-Fe-containing compositions, the calculated electronic structure with a wide minority band gap seems rather unrealistic. In the Co_2MnSi compound, the Fermi energy lies within the valence energy band, therefore half-metallicity ($P = 100\%$) is lost. This is in contradiction to the experimental observations in a Co_2MnSi -based MTJ [3], where the E_F is situated closer to the conduction band minimum. This indicates that the Coulomb-exchange parameter depends on the Fe concentration and it is less dominant in the $x \geq 0.5$ composition interval. This is the region, indeed, where the simple GGA approach is also efficient for predicting the total magnetization, as is shown in figure 4(a).

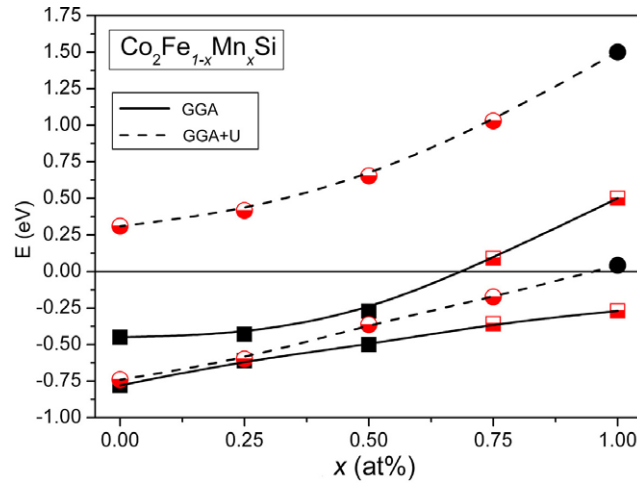


Figure 5. The position of the minority band gap for $\text{Co}_2\text{Fe}_{1-x}\text{Mn}_x\text{Si}$ alloys with $L2_1$ structure calculated within the GGA and GGA + U theorems, respectively.

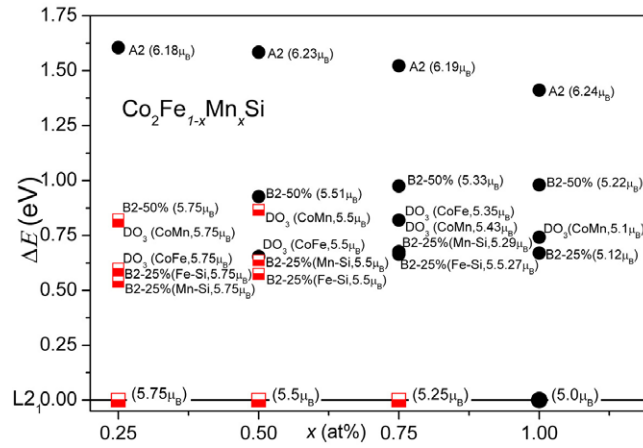


Figure 6. The effect of alloying and the effect of various disorders for the half-metallicity in $\text{Co}_2\text{Fe}_{1-x}\text{Mn}_x\text{Si}$ alloys compared by their difference in total energy.

3.3. Quarternary $\text{Co}_2\text{Fe}_{1-x}\text{Cr}_x\text{Si}$ alloys

Figure 7 shows the spin-resolved DOS for the $\text{Co}_2\text{Fe}_{1-x}\text{Cr}_x\text{Si}$ alloys. In accordance with the above-described cases, when the number of valence electrons is reduced, this time by the Fe replacement for Cr, E_F is found to be deeper into the minority band gap and is situated around the middle of the gap for $x = 0.25$. When the Cr concentration is increased to $x = 0.5$, the maximum valence electron energy band becomes close to E_F , predicting a lower resistance of the half-metallicity against structural disorder. With further Cr substitution for Fe up to $x \geq 0.75$, E_F intercepts the valence electron energy bands and results in destroyed half-metallic properties (not shown here). In principle, the situation is similar to that of the series of $\text{Co}_2\text{Fe}_{1-x}\text{Mn}_x\text{Si}$ alloys; however, the Cr atom has two valence electrons fewer than the Fe atom, while this deficiency is only one for a Mn atom, thus the virtual replacement

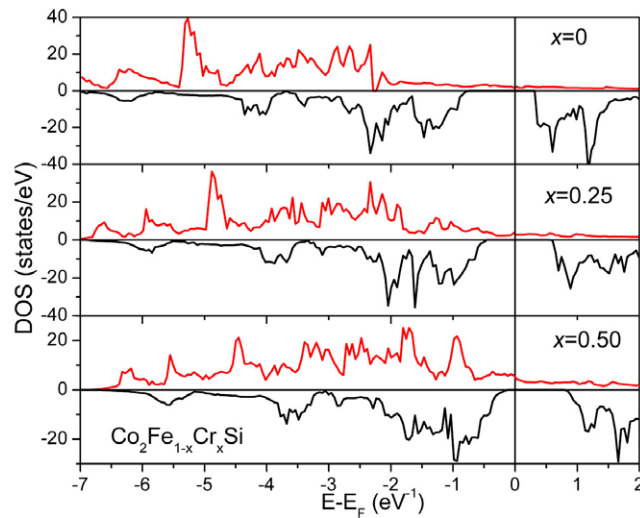


Figure 7. The effect of Cr addition on the total density of states in $\text{Co}_2\text{Fe}_{1-x}\text{Cr}_x\text{Si}$ calculated by the GGA + U model. A shift in the relative position of the Fermi level within the band gap is observed.

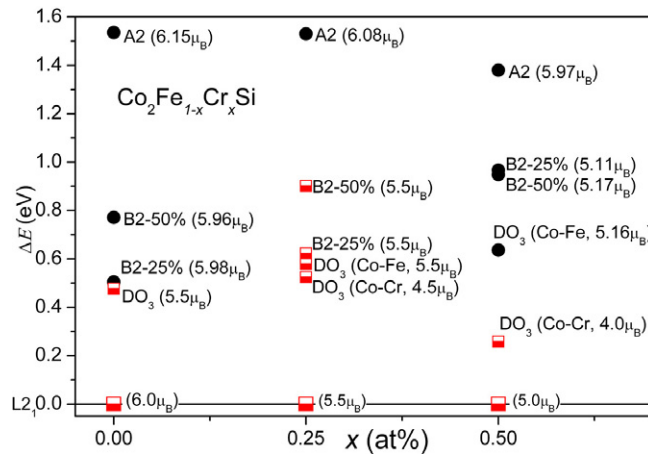


Figure 8. The effect of alloying and the effect of various disorders for the half-metallicity in $\text{Co}_2\text{Fe}_{1-x}\text{Cr}_x\text{Si}$ alloys compared by their difference in total energy. The central position of the Fermi level makes the composition with $x = 0.25$ a promising candidate as an electrode material in MTJs.

of E_F is more obvious by the same amount of x addition. This tendency is also observed for the change in magnetization with composition, as is shown in figure 4(b). Once again, the predicted magnetization using the GGA theorem differs from the Slater–Pauling rule for $x \leq 0.5$, and good agreement between the theories can be observed only for high-Cr-content alloys ($x \geq 0.5$). Experimental works show comparable results to the predictions made within the GGA + U framework; however, the compositions above $x \leq 0.3$ do not form single $L2_1$ structure, thus this tendency cannot be completely confirmed by experiment in the whole composition range [17]. For this reason, our investigations on the effect of disorder are restricted to $x \leq 0.5$ (see figure 8).

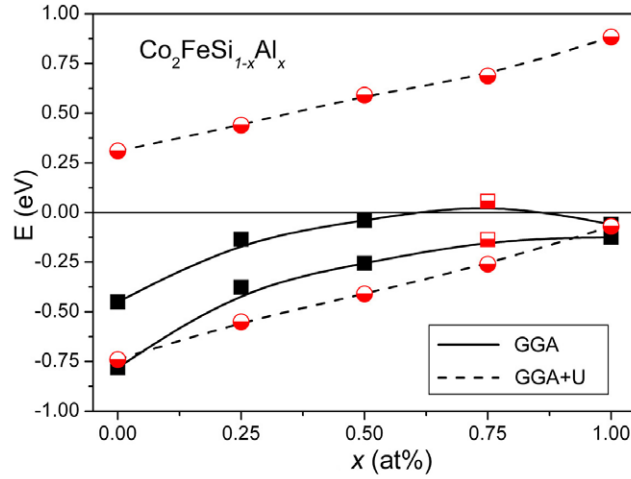


Figure 9. The position of the minority band gap for ordered $\text{Co}_2\text{FeSi}_{1-x}\text{Al}_x$ alloys calculated within the GGA and GGA + U theorems, respectively.

The half-metallicity is retained for neither case when the Co swaps site with the Fe or with the Cr atom. However, the alloy with 12.5% of Co–Fe disorder is just the edge of half-metallicity, so a wide gap (~ 0.56 eV) still exists when a change in the Co and Cr positions occurs. Interestingly, a steep decrease in the total magnetization to $4.5 \mu_B$ is also observed with this disorder, because the Cr atoms are aligned antiparallel with a small spin magnetic moment of $-0.34 \mu_B$. This behavior was also reported previously for the $\text{Co}_2\text{Fe}_{1-x}\text{Cr}_x\text{Al}$ alloys [27, 28]. As for the non-magnetic p-block element Si, its position at the 8a sublattice results in a completely destroyed gap at E_F , similar to the previously described compositions. The band gap due to the presence of B2-type disorder shrinks from ~ 0.98 to ~ 0.50 eV, but it still exists. The same tendency can be seen in the $\text{Co}_2\text{FeSi}_{0.5}\text{Al}_{0.5}$ alloy, as described below. The characteristic difference from this latter alloy, regarding the total energy values, is that the $L2_1$ phase is the most stable structure at 0 K.

3.4. Quarternary $\text{Co}_2\text{FeSi}_{1-x}\text{Al}_x$ alloys

Substitution of Al for Si in the $\text{Co}_2\text{FeSi}_{1-x}\text{Al}_x$ alloy also leads to a decrease in the total number of valence electrons (Z) because of the difference in valence electrons between Si ($3s^2 3p^2$) and Al ($3s^2 3p^1$). Again, the decline from Stoner–Pauling behavior for $x \leq 0.5$ is observed in the case of GGA theory, which is corrected by the on-site Coulomb exchange, as shown in figure 4(c).

As reported recently [15, 16], within the GGA + U theorem the band gap in the minority states can be engineered by changing the compositions of the $\text{Co}_2\text{FeSi}_{1-x}\text{Al}_x$ alloy. As shown in figure 9, the Fermi level lies at the higher end of the minority gap for Co_2FeSi calculated by GGA + U , while that of Co_2FeAl is at the lower edge. The most promising candidates are the $\text{Co}_2\text{FeSi}_{1-x}\text{Al}_x$ alloys with $0.25 \leq x \leq 0.75$, because their E_F lies deep in the band gap; therefore, their half-metallic properties may be more resistant against the structural disorder than the terminal alloys ($x = 0$ and 1). Interestingly, the GGA theory predicts a weak half-metallic nature of the compositions around $x = 0.75$ with the $L2_1$ structure. Unfortunately, no long-range-ordered structure could be achieved experimentally in the compositions above

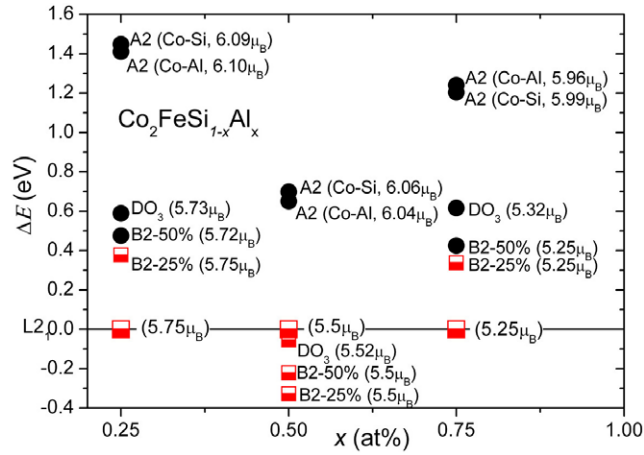


Figure 10. The effect of alloying and the effect of various disorders for the half-metallicity in $\text{Co}_2\text{FeSi}_{1-x}\text{Al}_x$ alloys compared by their difference in total energy. The $L2_1$ phase was found to be less stable comparing the total energies, than the partly B2 or DO_3 disordered phases for $x = 0.5$.

0.7 [16]. The effect of moderate A2-, DO_3 - or B2-type disorders on spin polarization in the composition range $0 \leq x \leq 0.75$ is presented in figure 10.

As in all the previous cases, the moderate disordering between Fe, Co and Si atoms forms additional electronic states near the gap edge in the case of $\text{Co}_2\text{FeSi}_{1-x}\text{Al}_x$, with $x = 0.25$, 0.5 and 0.75 (not shown here). In the equiatomic Al–Si concentration ($x = 0.5$), the half-metallicity is preserved for the B2 disordered states, because the newly formed energy states at both edges of the gap have less contribution to the Fermi level (figure 10). Further Al substitution to $x = 0.75$ results in a comparable half-metal response against the effect of disorder than that for $x = 0.25$. These calculations for the $x = 0.5$ alloy also revealed the unique character of this composition. The energetically most favorable structure is no longer the $L2_1$ structure but the partly (25% B2) disordered structure, considering the total energy values. Even the structures with the replacement of two Fe atoms by one Si atom and one Al atom (50% B2) or one Co atom by one Fe atom (12.5% A2 disordered) are more stable than the perfect $L2_1$ structure, considering the total energy values at the ground state. This finding presumes a lack of complete $L2_1$ order in real alloys at finite temperatures around this composition. It should be noted that the same tendency was observed independently whether the applied model was GGA or GGA + U .

3.5. Quarternary $\text{Co}_2\text{FeSi}_{1-x}\text{Ga}_x$ alloys

Finally, we gradually replaced Si by Ga ($3d^{10}4s^24p^1$) in the $\text{Co}_2\text{FeSi}_{1-x}\text{Ga}_x$ alloy to decrease the total number of valence electrons. The expected magnetic moment from the GGA model follows a linear dependence in the low-Si-content regime ($x \geq 0.75$); however, the GGA method does not result in integer ($5.00 \mu_B$) M_t but in a slightly higher value of $5.07 \mu_B$ (see figure 4(d)). This value reached an even higher $5.3 \mu_B$ when Coulomb exchange is introduced, which slightly overestimates the experimentally measured $5.13 \mu_B$ at 4.2 K [29]. Interestingly, the Slater–Pauling rule is predicted only by the GGA + U theory for compositions above $x < 0.75$, unlike the previous cases. The value of U was fixed during the calculations and its compositional dependence was not taken into account, which may be the reason for this

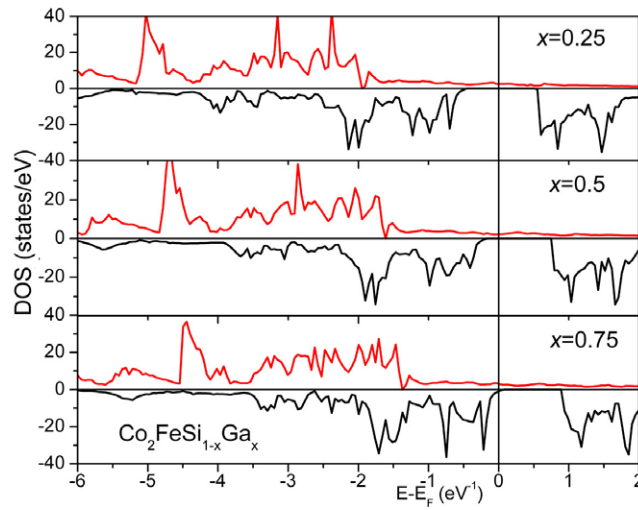


Figure 11. The effect of Ga addition on the total density of states of $\text{Co}_2\text{FeSi}_{1-x}\text{Ga}_x$ calculated by the GGA + U model. The composition with $x = 0.25$ is a promising candidate as an electrode material in MTJs.

deviation. Once again, as Z is decreased by more Ga addition for Si up to $x \geq 0.75$, the Fermi level is shifted over the band gap and it meshes with the valence band, resulting in lower P even in the $L2_1$ ordered state (figure 11). Therefore, our calculations to investigate the disorder effect are restricted to the composition range $0 \leq x \leq 0.5$. The most promising candidate from the $\text{Co}_2\text{FeSi}_{1-x}\text{Ga}_x$ series with spin polarization which is resistant against disorder is the $x = 0.25$ composition with E_F close to the middle of minority band gap (figure 12). As summarized in figure 13, only the A2-type intermix of Co with Si or with Ga destroys the half-metallicity. The scenario that the vacancy on the Si site would be more likely to be filled by Co than by Ga is rather improbable. When $x = 0.50$, only the $L2_1$ -ordered phase is predicted to be half-metallic, while half-metallicity is not observed for $x = 0.75$ and 1.

4. Summary and conclusions

We have comparatively studied the magnetic and half-metallic properties of several Co_2Fe -based ternary and quaternary alloys within the GGA and GGA + U theories. A weak Coulomb exchange can explain the experimentally observed magnetization for alloys with high Co and Fe content. We found that the lowering of M_S from $6 \mu_B$ in the Co_2FeSi alloy can be attributed to the presence of A2-type disorder, as reported in [7, 8]. A moderate change in the Co/Fe ratio can stabilize the half-metallicity, due to the change in the position of the Fermi energy within the minority band gap. An increase in the Co/Fe ratio results in a virtual breaking of the Slater–Pauling rule, because the substituted Co atoms act as DO₃-type disorder on the 4b sublattice and they carry a lower magnetic moment than the replaced Fe atoms. Therefore, chemical inhomogeneity or slightly off-stoichiometric compositions would also lead to a decrease in the observed M_t . One can expect an improvement in the experimentally measured value of P in these ternary alloys, if a very high degree of ordering is achieved. For the equiatomic $\text{Co}_2\text{FeSi}_{0.5}\text{Al}_{0.5}$ alloys, the lack of complete order, as well as the high expected spin polarization in the disorder state by the GGA + U , is also in good agreement with experimental results [21].

As for the quaternary $\text{Co}_2\text{Fe}_{1-x}\text{Mn}_x\text{Si}$ alloys, a small Coulomb exchange can reproduce the Slater–Pauling rule that was reported experimentally [14]; however, it results in

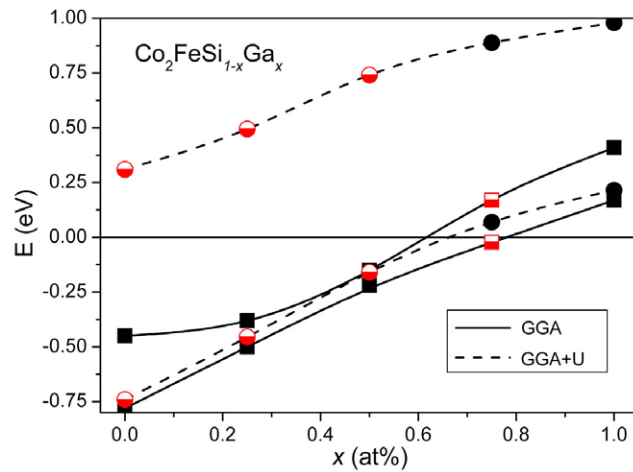


Figure 12. The position of the minority band gap for $L2_1$ -ordered $\text{Co}_2\text{FeSi}_{1-x}\text{Ga}_x$ alloys calculated within the GGA and GGA + U theories, respectively. The half-filled squares and circles represent $P = 1$, while full squares and circles indicate lower spin polarization than 100% ($P < 1$).

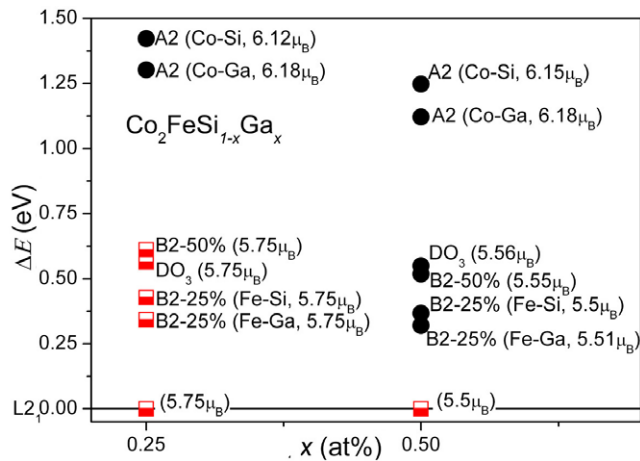


Figure 13. The effect of alloying and the effect of various disorders for the half-metallicity in $\text{Co}_2\text{FeSi}_{1-x}\text{Ga}_x$ alloys compared by their difference in total energy.

a contradiction in the Co_2MnSi alloy with no half-metallicity properties and a rather unrealistically wide band gap. This result, together with the fact that the total magnetization is as accurately predicted by the GGA theory for alloys $x \geq 0.5$, indicates that the electron repulsion is less dominant with decreasing Fe concentration and does not need to be considered within the whole composition range. This conclusion can also be drawn from the high-Ga-containing alloys.

Finally, this work shows that taking the on-site correlation into account is a key factor for the correct description of magnetic and electronic structure in the Co_2Fe -based Heusler alloys. Our investigations also suggest that there is a possibility of obtaining a material with high spin polarization, even in the presence of disorder; however, the A2-type disorder should be completely avoided.

Acknowledgment

This work was supported by the Special Coordination Funds for Promoting Science and Technology from the Ministry of Education, Culture, Sports, Science and Technology, Japan.

References

- [1] Kübler J, Williams A R and Sommers C B 1983 *Phys. Rev. B* **28** 1745
- [2] Kämmerer S, Thomas A, Hütten A and Reiss G 2004 *Appl. Phys. Lett.* **85** 79
- [3] Sakuraba Y, Hattori M, Oogane M, Ando Y, Kato H, Sakuma A, Kubota H and Miyazaki T 2006 *Appl. Phys. Lett.* **88** 192508
- [4] Inomata K, Okamura S, Miyazaki A, Kikuchi M, Tezuka N, Wojcik M and Jedryka E 2006 *J. Phys. D: Appl. Phys.* **39** 816–22
- [5] Gercsi Z, Rajanikanth A, Takahashi Y K, Hono K, Kikuchi M, Tezuka N and Inomata K 2006 *Appl. Phys. Lett.* **89** 082512
- [6] Galanakis I, Dederichs P H and Papanikolaou N 2002 *Phys. Rev. B* **66** 174429
- [7] Niculescu V *et al* 1977 *J. Magn. Magn. Mater.* **5** 60
- [8] Niculescu V *et al* 1979 *Phys. Rev. B* **19** 452
- [9] Wurhmel S *et al* 2005 *Phys. Rev. B* **72** 184434
- [10] Wurhmel S *et al* 2006 *J. Appl. Phys.* **99** 08J103
- [11] Wurhmel S *et al* 2005 *Phys. Rev. B* **72** 184434
- [12] Kandpal H C, Fecher G H, Felser C and Schönhense G 2006 *Phys. Rev. B* **73** 094422
- [13] Wurhmel S *et al* 2005 *Preprint cond-mat/0506729*
- [14] Balke B, Fecher G H, Kandpal H C, Felser C, Kobayashi K, Ikenaga E, Kim J-J and Ueda S 2006 *Phys. Rev. B* **74** 104405
- [15] Fecher G H and Felser C 2007 *J. Phys. D: Appl. Phys.* **40** 1582–6
- [16] Nakatani T M, Rajanikanth A, Gercsi Z, Takahashi Y K, Inomata K and Hono K 2007 *J. Appl. Phys.* accepted
- [17] Karthik S V, Rajanikanth A, Nakatani T M, Gercsi Z, Takahashi Y K, Inomata K and Hono K 2007 *Appl. Phys. Lett.* accepted
- [18] Tezuka N, Ikeda N, Sugimoto S and Inomata K 2006 *Appl. Phys. Lett.* **89** 252508
- [19] Galanakis I, Özdoğan K, Aktas B and Sasioglu E 2006 *Appl. Phys. Lett.* **89** 042502
- [20] Miura Y, Shirai M and Nagao K 2006 *J. Appl. Phys.* **99** 08J112
- [21] Picozzi S, Continenza A and Freeman A J 2004 *Phys. Rev. B* **69** 094423
- [22] <http://staff.aist.go.jp/t-ozaki/>
- [23] Deb A, Itou M, Sakurai Y, Hirakoa N and Sakai N 2001 *Phys. Rev. B* **63** 064409
- [24] Bandyopadhyay T and Sarma D D 1989 *Phys. Rev. B* **39** 3517
- [25] Solovyev I V and Imada M 2005 *Phys. Rev. B* **71** 045103
- [26] Cox B N, Coulthard M A and Lloyd P 1976 *J. Phys. F: Met. Phys.* **4** 807
- [27] Miura Y, Nagao K and Shirai M 2004 *Phys. Rev. B* **69** 144413
- [28] Fecher G H, Kandpal H C, Wurhmel S, Morais J, Lin H-J, Elmers H-J, Schönhense G and Felser C 2005 *J. Phys.: Condens. Matter* **17** 7237–52
- [29] Buschow K H J and Van Engen P G 1981 *J. Magn. Magn. Mater.* **25** 90